Spectral Interferometry for TSV Metrology in Chiplet Technology

Stefan Schoeche*[a], Daniel Schmidt[a], Junwon Han[a], Shahid Butt[a], Katherine Sieg[a], Marjorie Cheng[b], Aron Cepler[b], Shaked Dror[c], Jacob Ofek[c], Ilya Osherov[c], and Igor Turovets[c]
[a]IBM Research, 257 Fuller Road, Albany, NY 12203, USA
[b]Nova Measuring Instruments Inc., 3342 Gateway Blvd, Fremont, CA 94538, USA
[c]Nova Ltd., 5 David Fikes St., Rehovot, 7632805, Israel

ABSTRACT

Comprehensive through-silicon-via (TSV) characterization, including grind side measurements, is critical to ensure device reliability in chiplet technology. Here we report on TSV metrology using spectral interferometry (SI), which is used to acquire absolute phase information of polarized and broad-band light interacting with a sample. This phase information can be translated into the optical path length of the partial beams traveling within the structure. We utilize the spatial separation of peaks related to light reflected from the top surface and the surface of interest to directly measure the TSV depth after reactive ion etching as well as the reveal height on the grind side, without modeling and even in the presence of multilayers or surrounding patterning. Polarization-dependent SI measurements enable the quantification of asymmetry at the bottom of the TSVs not visible in top-down CD measurements. SI is robust and fast and unveils novel information in TSV metrology not accessible with established in-line metrology techniques.

Keywords: Through-Silicon-Vias, Spectral Interferometry, Metrology

*Corresponding author: sschoeche@ibm.com

1. INTRODUCTION

Chiplet technology enables full 3D integration for faster, more energy-efficient computation and heterogenous integration to lower cost [1]. Through-silicon-vias (TSV) enable chiplet technology by providing access to the backside of the chip. Current TSV dimensions present several challenges for full characterization using established in-line metrology techniques [2]. For example, the TSV diameter, depth, and pitch are too large to apply NIR-UV scatterometry. Only top CD information is accessible from CDSEM or optical microscopy. Visible-light reflectometry can measure the TSV depth on isolated TSVs but becomes challenging in the presence of multiple layers or patterning surrounding the TSVs [2]. Advanced techniques such as X-ray tomography or infrared and THz reflectometry from the wafer backside are not suitable for in-line metrology [2]. Time-domain interferometry is commonly applied for TSV depth measurements but is relatively slow due to reference mirror movement and limited in terms of the applicable minimum TSV diameters [3].

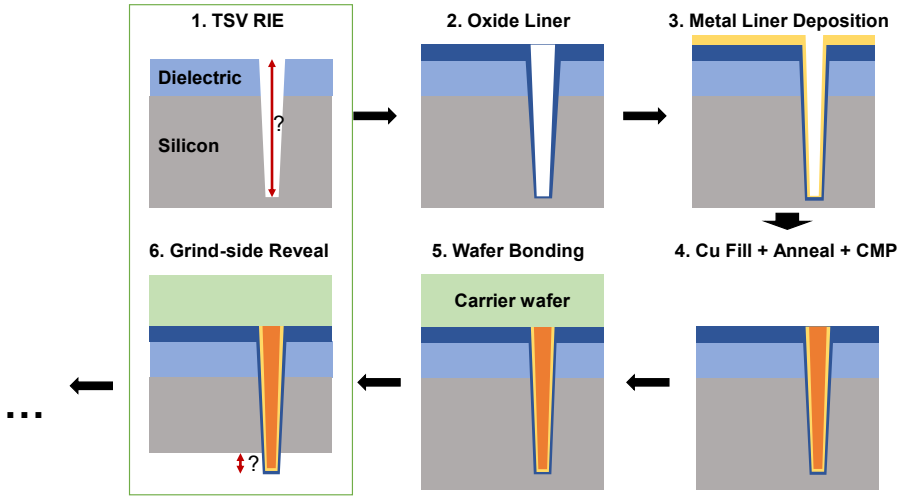

Figure 1. Sequence of the standard TSV process flow consisting of TSV RIE, oxide liner deposition, metal liner deposition, Cu fill/annealing/overburden CMP, wafer bonding to a carrier wafer, and grind-side reveal.

Metrology, Inspection, and Process Control XXXVIII, edited by Matthew J. Sendelbach, Nivea G. Schuch, Proc. of SPIE Vol. 12955, 129551O · © 2024 SPIE
0277-786X · doi: 10.1117/12.3011748

The main processing steps in the TSV process flow are depicted in Fig. 1. Two out of several critical parameters of interest are the depth of the TSV after the reactive ion etching (RIE) step and the reveal height of the TSV tip after wafer bonding and grind-side reveal. A robust and non-destructive measurement technique is required to access these critical parameters. Here, we explore Spectral Interferometry (SI) as a fast and reliable metrology approach to measure these two parameters in the TSV process flow while also delivering valuable information about structural asymmetry at the TSV bottom.

2. EXPERIMENTAL DETAILS

We employ the Nova Prism tool which combines spectral reflectometry data with SI capabilities. The polarized SI channels utilize a fixed reference surface with a sophisticated optical path design to provide spectra in the frequency domain. From these spectral data, absolute phase signals can be extracted to complement the polarized reflectometry data and greatly enhance sensitivity of the tool for OCD applications [4]. In combination with innovative algorithms, access to the absolute phase information further enables some unique capabilities absent in alternative OCD tools. Filtering the phase data can remove contributions from a complicated multilayer stack or patterned layers. This simplifies the analysis to only the geometry of interest at the top of the sample [5]. The same data can be utilized to identify characteristic contributions of particular interfaces of interest, such as the sample surface or the bottom of a TSV. A Fourier transformation of the phase signal provides a unique representation of the data in terms of the optical path length (OPL) traveled by the probing light. Each interface in the layer stack creates characteristic peaks in the interferograms. The OPL difference between peaks from interfaces of interest and their height allows us to directly measure geometrical dimensions, such as the depth of a TSV, without the need for optical modeling.

For this study, standard 300 mm Si wafers were processed following the steps in Fig. 1. Short-loop wafers that only contained TSVs etched into Si wafers coated with only a dielectric layer, but no other layers or patterning, as well as wafers with full back-end processing, were investigated. Asymmetric processing can occur during the TSV RIE process, especially towards the wafer edge [6]. Figure 2 depicts the resulting TSV geometry resulting from asymmetric processing. Typically, the TCD is much less affected by this non-ideality than the bottom of the TSV. Thus, this misprocessing is hard to detect using top-down imaging methods such as optical microscopy or even CD-SEM, for example. The Prism tool can measure SI with different polarization states, and a minimum of two orthogonal-polarization measurements are applied to reveal the presence of TSV bottom asymmetry.

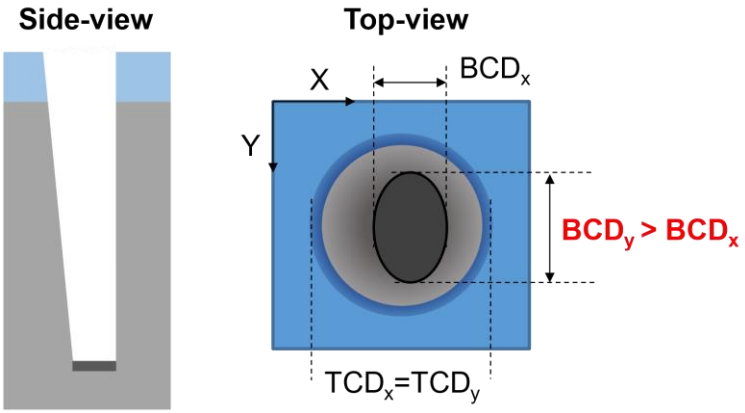

Figure 2. Schematic side- and top-view of a TSV etched into a dielectric-coated Si wafer resulting from asymmetric processing. The TSV bottom within the Si wafer is marked in dark grey.

3. RESULTS AND DISCUSSION

A schematic representation of the SI signal as a function of the OPL traveled by the probing light is shown in Fig. 3 for a TSV short loop that only contained the TSVs etched into a dielectric-coated Si wafer. A schematic drawing illustrates the path traveled by the partial waves probing the sample (with multiple reflections within the dielectric omitted for clarity). If a wavefront hitting the surface of the sample is considered, part of that light will be reflected and reach the detector at

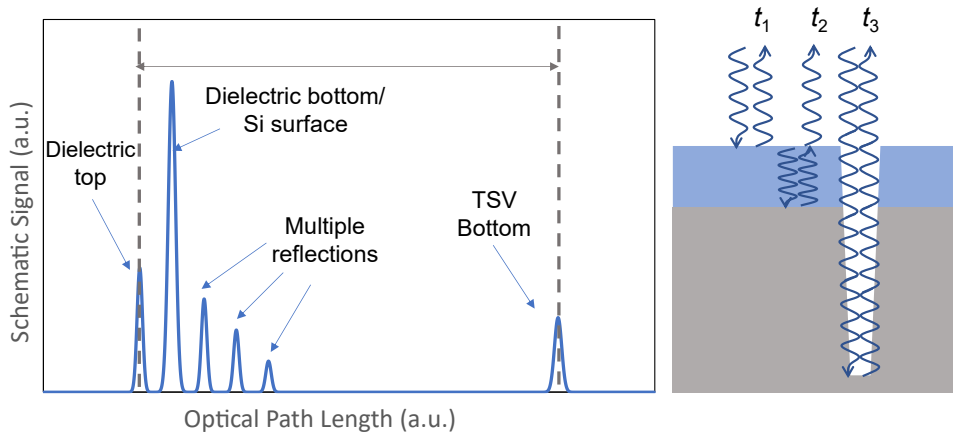

Figure 3. Schematic representation of the SI data for measurements on an individual TSV on short-loop wafer containing only TSVs etched into a dielectric-coated Si wafer. Contributions from different interfaces are indicated in the graph along with the optical path length difference between the top surface and TSV bottom peak used to extract the TSV depth. The illustration shows partial waves contributing to the SI signal.

time t_1. A peak related to this top surface reflection will appear in the SI data at the shortest OPL value. Some light will transmit through the top surface, reflect off the dielectric-substrate interface, and reach the detector after time t_2 which results in the highest peak to the right of the dielectric top surface peak. Multiple reflections within the dielectric layer create equally spaced peaks of declining amplitude. The waves reaching the TSV bottom travel a much longer distance before being detected at time t_3. The according TSV bottom peak appears in the SI data as a single isolated peak far off from the surface reflection peaks (Fig. 3). Since the measurement spot size is larger than the TSV top CD, all signal contributions are collected in a single, fast measurement. The ratio of the OPL and the refractive index n of the transmission material gives the distance traveled by individual partial waves:

$$d = {}^{\mathrm{OPL}}/_{n}\,. \tag{1}$$

The depth of the TSV can easily be extracted as half of the OPL difference between the top surface peak and the TSV bottom peak since the light travels down the TSV and back up and is transmitted through air ($n = 1$). Note that no sophisticated model approach is required to measure this TSV depth directly from the SI data. The SI data from the Nova Prism tool provides excellent depth resolution suitable for measuring small TSV depth of a few tens of microns up to several hundreds of microns for TSV diameters of microns up to several tens of microns. The tool's capabilities to extract even smaller TSV dimensions anticipated for future applications are not limited, as conventional OCD model approaches can be applied once this simple depth extraction algorithm proves to be no longer accurate. Radial distribution and wafer map data for a typical short-loop wafer are shown in Fig. 4 (a) and Fig. 4 (b) exemplifying the robust extraction of the TSV depth without outliers.

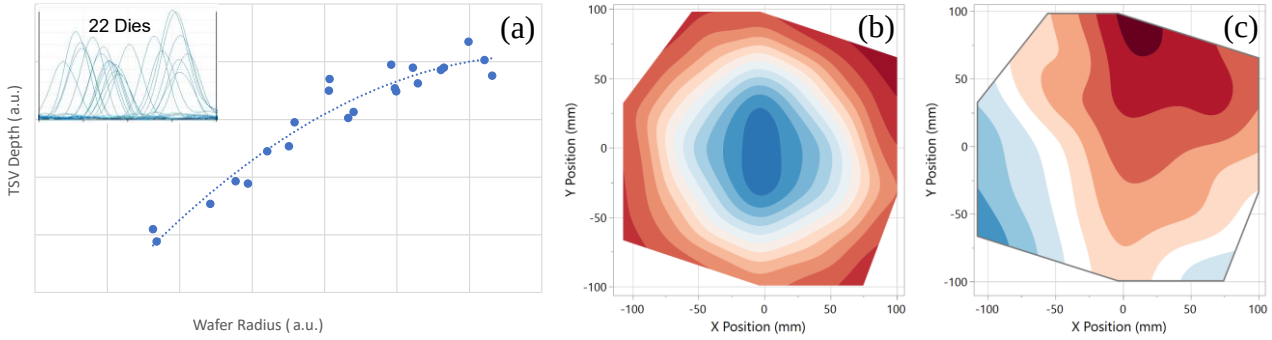

Figure 4. Radial distribution (a) and a wafer map (b) of the extracted TSV depth on a short-loop wafer measured on 22 dies. Actual measurement data for the TSV bottom peaks is shown in the insert in (a). In addition, the dielectric blanket layer thickness around the top of the TSV is shown (c).

The excellent depth resolution of the tool allows the extraction of additional information, such as the thickness of the dielectric blanket layer surrounding the TSV top, by considering the OPL difference between the top surface peak and the dielectric-substrate interface peak. In this case, a nominally 2 µm thick dielectric layer was present on the wafer, and the wafer map of the extracted dielectric blanket thickness is shown in Fig. 4 (c). Note that this measurement approach can be applied to isolated TSVs and dense arrays of TSVs. In the latter case, the bottom peak will be higher since more TSVs reflect light back, but the peak position does not change.

A major advantage of the SI technique is its applicability to full-flow wafers with complicated multilayer structures and patterned features near the TSV. Figure 5 (a) shows a schematic representation of SI data for a wafer with full back-end processing. Several layers and patterning near the TSV create an intricate surface interference pattern. Nonetheless, the TSV bottom peak is isolated from the interference pattern and unaffected. Thus, even for a very complex geometry, the TSV depth can easily be extracted. Experimental results are shown in Fig. 5 (b).

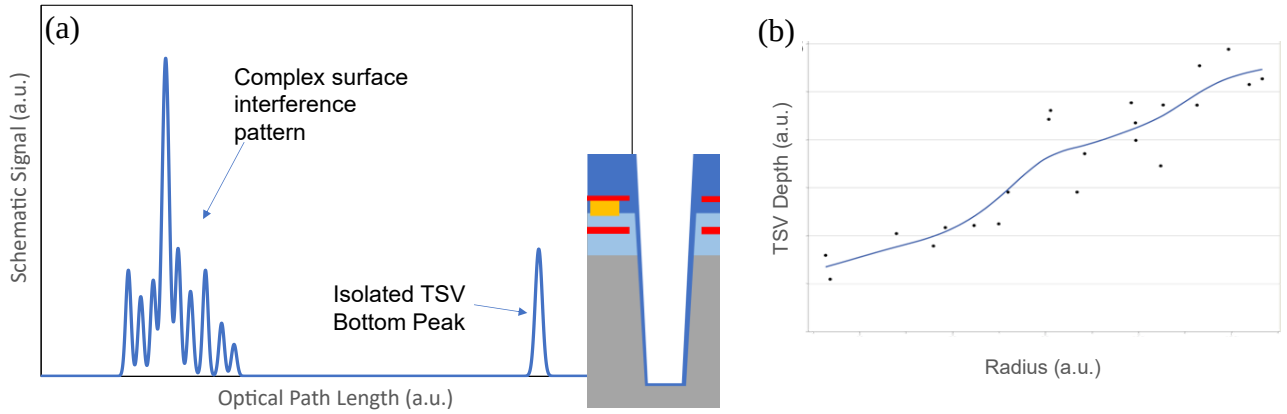

Figure 5. (a) Schematic representation of SI data for measurements on an individual TSV on a wafer with full back-end processing. Several layers and patterning in close proximity to the TSV create a complex surface interference pattern. However, the TSV bottom peak is entirely isolated from the surface interference pattern. (b) Radial distribution of the extracted TSV depth of a wafer with full backend processing.

Another critical parameter in the TSV process is the reveal height on the grind side. An illustration defining the reveal height parameter of the TSV pillar after grinding of the Si wafer and subsequent reveal etch is depicted in Fig. 6 (a). A schematic representation of the SI data for measurements on an individual TSV is shown in Fig. 6 (b). The probing light first interacts with the pillar top before reaching the ground-down Si surface. The peak associated with the protruding pillar top thus appears on the left side of the Si surface peak. Nonetheless, the data analysis is very similar to the depth measurement case, i.e., the total reveal height is given as half the OPL difference between the TSV pillar top peak and the Si surface peak.

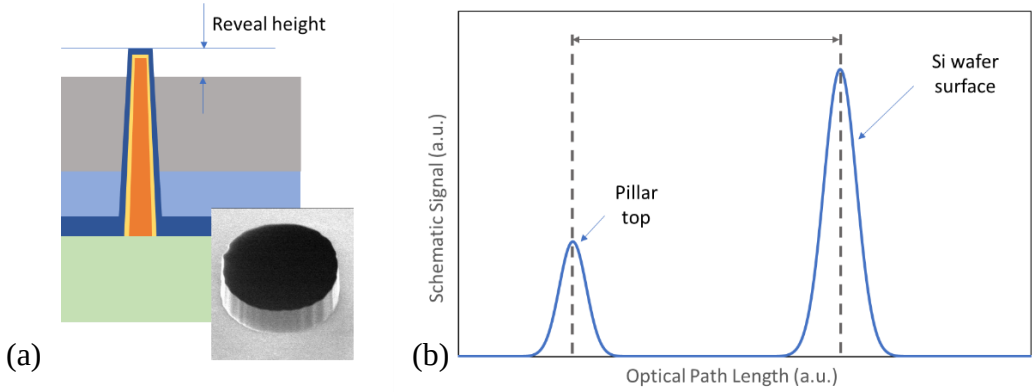

Figure 6. (a) Illustration of the reveal height of the TSV pillar on the grind side. A tilted-beam SEM image displays the TSV pillar after reveal viewed from the grind side. (b) Schematic representation of the SI data for measurements on an individual TSV pillar revealed on the grind side.

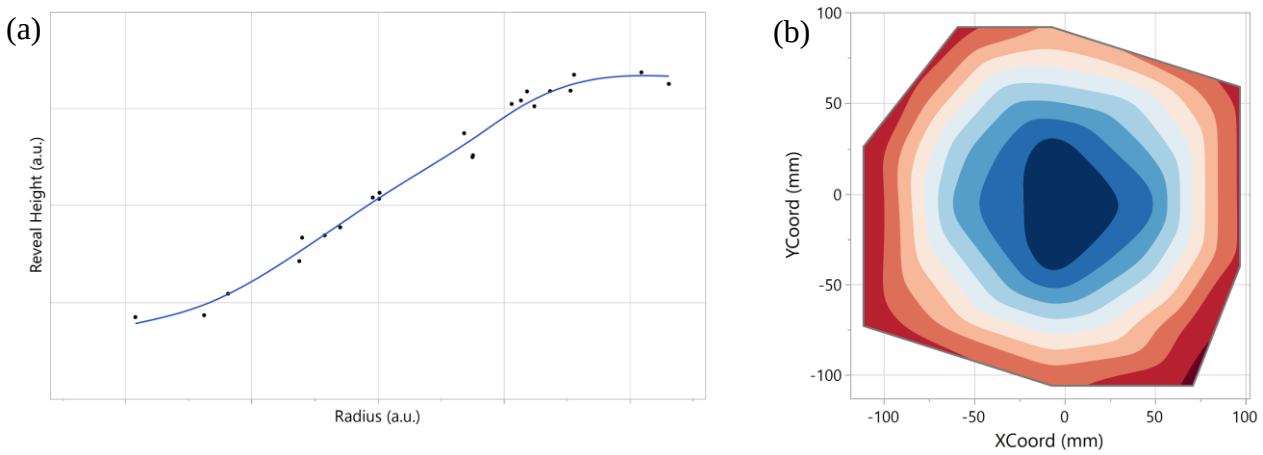

Figure 7. Radial distribution (a) and a wafer map (b) of the extracted TSV reveal height for a measurement on the grind side of a TSV short-loop wafer.

Radial distribution and the according wafer map for a TSV short-loop wafer demonstrate the robust extraction of the reveal height (Fig. 7). Typically, SI measures with a spot size larger than the TSV pillar diameter. Thus, a single, fast measurement provides the information of interest, and the spot size of the instrument does not limit the minimum applicable TSV diameter range. Further, the measurement is very tolerant to alignment inaccuracies, i.e., as long as the TSV pillar is situated within the measurement spot, the reveal height can be determined accurately.

A unique capability of the SI channel on the Nova Prism tool is the measurement of different polarization states, which can be exploited to detect and characterize feature asymmetry. Asymmetric processing can occur during the TSV RIE process, especially towards the wafer edge (Fig. 2). As an approximation, it is assumed that the asymmetry can be described as an elliptical distortion of the otherwise round TSV bottom (Fig. 8). The orientation of the bottom ellipse is expected to change along the wafer edge with tangentially oriented major axis, i.e., the minor axis points towards the wafer center. An asymmetry parameter A can be defined as the weighted difference between the major and minor axes of the TSV bottom ellipse. If the major and minor axes are aligned horizontally or vertically, the asymmetry parameter A is defined as:

$$A = \frac{R_V - R_H}{(R_V + R_H)/2} \tag{2}$$

Some of the processed TSV wafers exhibited a difference in the TSV bottom peak intensity on the very edge of the wafer for measurements with orthogonal polarization states. This difference can be used to measure the asymmetry parameter optically. The measured optical asymmetry depends on the orientation of the TSV bottom ellipse, with maximum asymmetry occurring when the polarization axes are aligned with the major and minor axes of the TSV bottom ellipse.

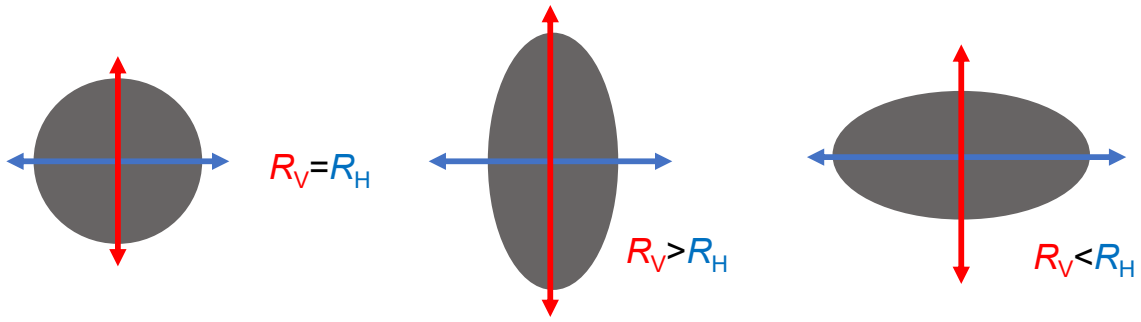

Figure 8. Approximation of the TSV bottom shape for perfectly round, i.e. symmetric, and elliptically distorted, i.e. asymmetric, cases. R_V and R_H are the major or minor axis of the ellipses oriented in vertical and horizontal direction, respectively.

A wafer map of the optically determined asymmetry parameter is shown in Fig. 9. This map was obtained with horizontal and vertical polarizations for each measurement spot on the wafer. The expected shape and orientation of the TSV bottom at the center and the bottom and left edges of the horizontal and vertical axes of the wafer are overlayed to the measurement data. Significant optical asymmetry is observed only at the very edge of the wafer, with negative values on the vertical axis and positive values on the horizontal axis, confirming expectations. On the diagonals, the optical asymmetry vanishes despite the likely presence thereof at the edge, indicating that for a tilted bottom asymmetry relative to the probing polarizations, it is impossible to distinguish between no asymmetry or tilted asymmetry. To probe the shape and orientation of a randomly oriented asymmetric TSV bottom, measurements can be performed with varying orthogonal polarization orientations depending on the measurement position on the wafer, or a second measurement can be acquired after rotating the wafer by 45°, for example.

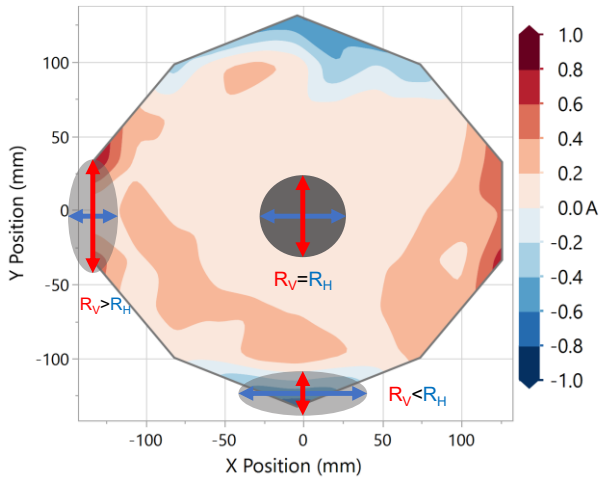

Figure 9. Wafer map of the optically determined asymmetry parameter *A* for measurements after the TSV RIE step. The expected shape and orientation of the TSV bottom at the center and the edges of the horizontal and vertical axes of the wafer are overlayed to the measurement data.

To confirm the bottom asymmetry, the optical asymmetry parameter was measured at the TSV RIE step for a dedicated wafer that was subsequently processed to the grind side reveal step, where the TSV bottom is revealed and can be inspected with optical or electron beam methods. SEM images were obtained for this wafer and analyzed with image analysis software to fit a best-matching ellipse to a feature in an image. That best-matching ellipse is shown for the center, top, bottom, left, and right dies on the test wafer overlayed on top of the measured asymmetry parameter map (Fig. 10). The map was mirrored on the vertical axis to account for the fact that the asymmetry parameter was measured from the wafer front side.

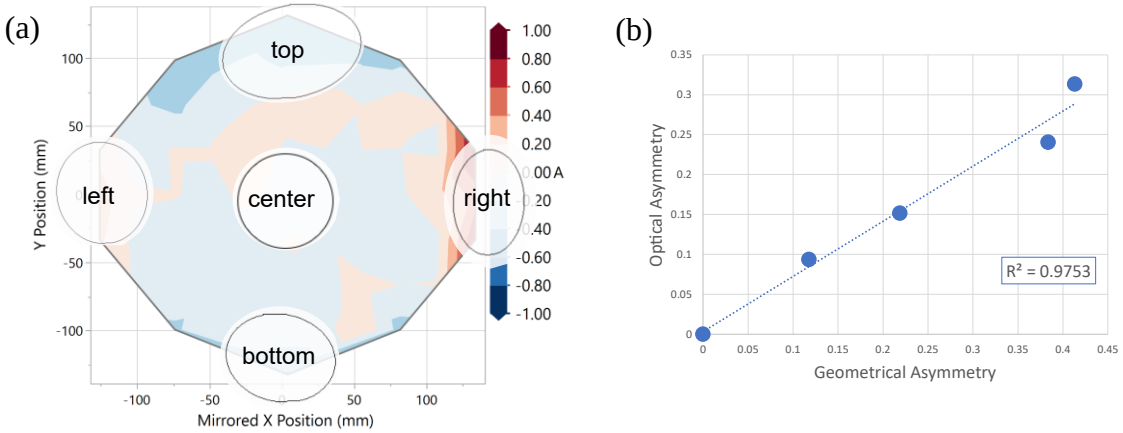

Figure 10. (a) Wafer map of the optically determined asymmetry parameter *A* for measurements after the TSV RIE step and best-matching ellipses of the TSV bottom matched to electron beam images of the TSV bottom at the grind-side reveal step. (b) Correlation of the optically determined asymmetry parameter and the actual geometric asymmetry obtained for the five test spots in (a).

The best-matching TSV bottom ellipses show the radial alignment as presumed, i.e., minor axis point towards the wafer center, and the most significant geometrical asymmetry values coincide with the largest values for the optical asymmetry. Linear correlation with an excellent R^2 is obtained when plotting the optically determined asymmetry parameter versus the geometrical asymmetry. This demonstrates that the polarization-dependent measurements reveal the geometrical asymmetry at the TSV bottom and can be used to quantify this parameter immediately after the TSV is formed.

4. SUMMARY AND CONCLUSIONS

SI enables the measurement of critical parameters in the TSV process flow. The distance between interfaces of interest can be extracted without modeling by representing the SI data in terms of the OPL traveled by the probing light. The OPL difference between peaks associated with these interfaces directly measures that distance. After TSV RIE, the TSV depth can be measured for a wide range of TSV diameters and depths by considering the OPL difference between the sample surface peak and the TSV bottom peak. This approach applies to fully integrated and short-loop wafers. At the grind-side reveal step, accurate and fast measurements of the TSV reveal height are enabled by measuring the OPL difference between the TSV pillar top peak and the Si surface peak. Polarization-dependent SI measurements are sensitive to geometrical asymmetry. Detection of TSV bottom asymmetry not visible with alternative metrology techniques is demonstrated and confirmed by comparison of the optically determined asymmetry parameter to the geometrical asymmetry parameter derived from best-matching ellipses matched to electron beam inspection data for the revealed TSV bottoms at the grind-side reveal step. The shape and orientation of a randomly oriented asymmetric TSV bottom can be determined by measuring with varying orthogonal polarization orientations or by performing multiple measurements with wafer rotation.

In conclusion, SI provides a fast and robust metrology solution for isolated and dense high-aspect ratio features such as TSVs without modeling and including unique information about feature asymmetry.

Acknowledgements

The authors would like to thank Hemanth Jagannathan, Mukta Farooq, Dale McHerron, Jennifer Oakley, Luciana Meli, Connor Franzese, Brian Seeley, and Chris Bottoms for fruitful discussions and support of this work.

REFERENCES

[1] S. Skordas, “The evolution of heterogeneous integration and packaging for the age of chiplets”, Proc. SPIE 12497, Novel Patterning Technologies, 1249702 (2023).
[2] J.P. Gambino, S.A. Adderly, J.U. Knickerbocker, “An overview of through-silicon-via technology and manufacturing challenges”, Microelectronic Engineering, Vol. 135, pp. 73-106 (2015).
[3] K. Sieg, C. Bottoms, C.J. Waskiewicz, A. Matos Mejia, J. Han, S. Butt, D. Schmidt, S. Schoeche, A. Hamer, A. Hubbard, “Large feature wafer level in-line optical metrology techniques for advanced packaging schemes”, Proc. SPIE 12955, Metrology, Inspection, and Process Control XXXVIII, 12955-57, (2024).
[4] D. Schmidt, C. Durfee, S. Pancharatnam, M. Medikonda, A. Greene, J. Frougier, A. Cepler, G. Belkin, D. Shafir, R. Koret, R. Shtainman, I. Turovets, and S. Wolfling, “OCD enhanced: implementation and validation of spectral interferometry for nanosheet inner spacer indentation”, Proc. SPIE 11611, Metrology, Inspection, and Process Control for Semiconductor Manufacturing XXXV, 116111U (2021).
[5] D. Schmidt, M. Medikonda, M. Rizzolo, C. Silvestre, J. Frougier, A. Greene, M. Breton, A. Cepler, J. Ofek, I. Kaplan, and R. Koret, “Spectral interferometry for fully integrated device metrology”, J. Micro/Nanopattern. Mats. Metro. 22(3), 031203 (2023).
[6] I. Seong, J. Lee, S. Kim, Y. Lee, C. Cho, J. Lee, W. Jeong, Y. You, and S. You, “Characterization of an etch profile at a wafer edge in capacitively coupled plasma”, Nanomaterials, 12(22), p.3963 (2022).